Stability and Photodynamics of Lumichrome Structures in Water at Different pHs and in Chemical and Biological Caging Media

ARTICLE *in* THE JOURNAL OF PHYSICAL CHEMISTRY B · FEBRUARY 2011

Impact Factor: 3.3 · DOI: 10.1021/jp110134f · Source: PubMed

THE JOURNAL OF PHYSICAL CHEMISTRY B

ARTICLE

pubs.acs.org/JPCB

Stability and Photodynamics of Lumichrome Structures in Water at Different pHs and in Chemical and Biological Caging Media

Maria Marchena,[†,‡] Michał Gil,[†] Cristina Martín,[†] Juan Angel Organero,[†] Francisco Sanchez,[‡] and Abderrazzak Douhal*[,†]

[†]Facultad de Ciencias Ambientales y Bioquímica, and INAMOL, Departamento de Quimica Fisica, Universidad de Castilla-La Mancha, Avenida Carlos III, S.N. 45071 Toledo, Spain.

[‡]Facultad de Quimica, Departamento de Quimica Fisica, Universidad de Sevilla, Calle Profesor Garcia Gonzalez, S.N. 41012 Sevilla, Spain.

Supporting Information

ABSTRACT: We report on photophysical studies of lumichrome (Lc) in water at different pHs, and interacting with the human serum albumin (HSA) protein and β-cyclodextrin (β-CD) in neutral aqueous solutions. We used steady-state and picosecond time-resolved emission spectroscopy to investigate the structural changes of Lc at the ground and excited states, as well as the rotational dynamics of the complexes with HSA and β-CD. In neutral water, the predominant neutral alloxazine-type structure of Lc coexists with a small population of the anionic form. In the presence of HSA, we observed an increase in the absorption band intensity at 450 nm. This increase is due to a preferential complexation (1:1 stoichiometry, K = 8600 M^{-1}) of the Lc anion structures within the protein. This change is not observed when β-CD is added, in which the Lc neutral form is exclusively complexed, giving a 1:1 stoichiometry. The fluorescence lifetimes of Lc in neutral water solutions are 4.2 and 2.3 ns, assigned to anionic and neutral alloxazinic forms, respectively. Using β-CD, the lifetime of the 1:1 complexes is 0.74 ns, while in the case of HSA complexes we observed two lifetimes (0.83 and 0.14 ns), which we explained in terms of different interactions of the anions with the protein. The rotational relaxation time of free Lc in neutral water is 75 ps. For Lc:β-CD complexes this time is 0.44 ns, in full agreement with the expected value from the hydrodynamic theory. For HSA solutions, we obtained a distribution of values between ~1 and 4.5 ns, suggesting a site heterogeneity of complexation and a different strength of binding for the involved Lc anionic forms. Our results give information about the different photorelaxation behavior of Lc within chemical and biological cavities, and might help in a better design of nanosystems for drug carriers and delivery.

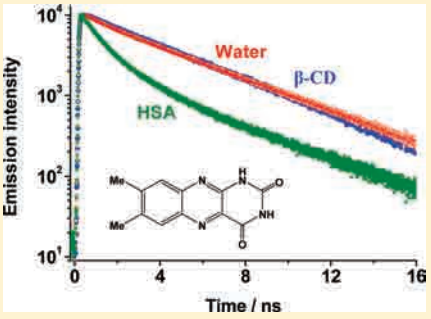

1. INTRODUCTION

The photophysics and photochemistry of flavins have been extensively studied as they are used as cofactors in enzymatic functions of flavoproteins.[1−3] The special role of the flavins derives from the unique ability of the isoalloxazine ring to mediate one- or two-electron-transfer steps between biological redox centers.[4,5] The major product of the decomposition and biodegradation of riboflavin (vitamin B_2) is lumichrome (Lc, 7,8-dimethylalloxazine). Lc is a nontoxic molecule and has some natural biological functions,[6−10] but in contrast to flavins, it does not show catalytic activity as a cofactor compound. The main biochemical interest in Lc, and alloxazines in general, was focused on their abilities as photosensitizers to generate singlet oxygen.[11−14]

Lc possesses an alloxazine scaffold unsubstituted at N-1 position (DMAL form, Scheme 1), which can undergo a tautomerization process involving N-1 and N-10 nitrogen atoms. This process gives an isoalloxazine-type structure (7,8-dimethylisoalloxazine, DMIS form). Intermolecular hydrogen bond (H-bond) formations with pyridine derivatives or with acetic acid were found to promote tautomerization via a photoinduced proton-transfer reaction at the electronically excited state.[15,16] Strong H-bond acceptor anions (like fluoride and acetate) or curcurbit[7]uril are able to facilitate the tautomerization of Lc at the ground state.[17,18] The possibility of existence of both tautomers in water has been ruled out by some authors, and a single lifetime was observed using time-resolved emission spectroscopy.[11,16,19,20] Other studies have suggested the presence of both (DMAL and DMIS) tautomers in aqueous solution.[21] Recently, a single fluorescence band and the lack of excited-state proton-transfer (ESPT) reaction to the solvent have been reported for the parent riboflavin molecule, as well as for flavin mononucleotide.[22,23] An intense isoalloxazine emission is observed in the solid lumichrome crystals, which is explained in

Received: October 22, 2010
Revised: December 17, 2010
Published: February 18, 2011

Scheme 1. (A) Schematic Representation of the Molecular Structures of Neutral and Anionic Forms of Lumichrome, Lc,[a] and (B) Views of the 1:1 Inclusion Complex between Lc and β-CD

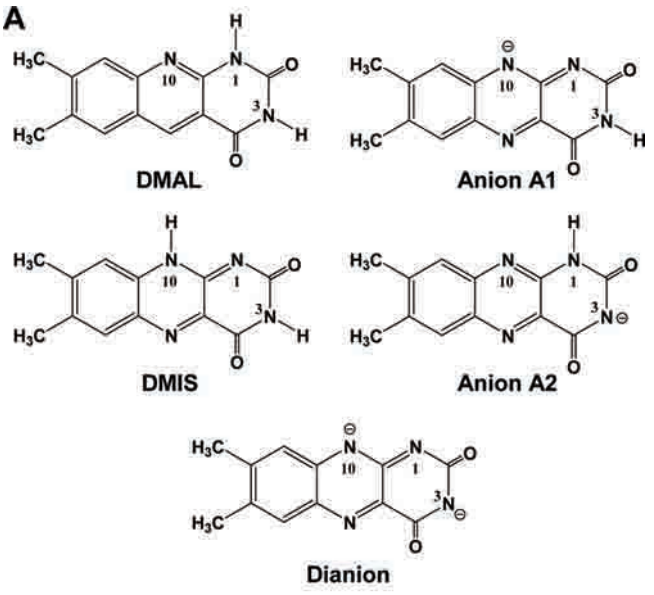

[a] DMAL = 7,8-dimethylalloxazine, DMIS = 7,8-dimethylisoalloxazine.

terms of an emission from doubly H-bonded dimers.[24,25] Some flavoproteins have the flavin moiety covalently bonded to the apoprotein. However, the majority of them contain the flavin noncovalently bound.[26] Recently, the binding of lumichrome to dodecins, a small flavoprotein, has been studied by fluorescence spectroscopy and X-ray crystallography.[27] The quaternary structure of dodecin consists of a dodecameric complex making a hollow sphere-like shape, where complexation of flavins occurs with 1:1 stoichiometry. The study shows that Lc has a high affinity to dodecin.

Therefore, we decided to investigate noncovalent interactions of Lc with the human serum albumin (HSA) protein, one of the most abundant proteins in the blood circulatory system. Recently, we have reported on the binding time and space domain characteristic of HSA with several molecules and drugs.[28−34] Our results showed that depending on the nature of the guest, we observed binding constants in buffered aqueous solution (pH ~7) ranging from 10^5 to 10^6 M^{-1}, and 1:1 or 1:2 (host:guest) stoichiometries. We also demonstrated that the caged guest in one of the hydrophobic pockets (see below) might have some restricted rotation within the protein, while in other cases, the produced complex is robust, reflecting the large affinity of the protein to this kind of guests.[34,33] We notice also that upon complexation with the protein the guest might change its conformation yielding a different structure from that stable in water. Crystallographic studies of HSA indicate that at pH 7, the protein adopts a heart-shape three-dimensional structure with three homologous α-helical domains I−III and a single tryptophan (Trp 214).[35−37] Each domain contains 10 helices and is divided into antiparallel 6-helix and subdomains (A and B). The ligands bind to HSA in regions located in the hydrophobic cavities of subdomains IIA (binding site I) and IIIA (binding site II). Binding to site I is dominated by the strong hydrophobic interactions with neutral heterocyclic compounds, while binding to site II involves ion(dipole)-dipole, van der Waals, and/or H-bonding interactions with the polar cationic groups of HSA.[35,37,38]

This report provides and discusses the results of studying the interactions of the Lc with the hydrophobic sites of HSA protein and compares them with those using the hydrophobic pocket of β-cyclodextrin (β-CD). As a reference, we studied the behavior of various structures of Lc in water at different pHs. The observed different behavior of Lc interacting with these cavities suggests that HSA and β-CD preferentially bind to different forms of the dye. The Lc anion is more stabilized in the presence of HSA, while for β-CD complex only the neutral DMAL structure is interacting. The results clearly show a different uptake of Lc by these hosts. Thus, we belive that our findings might be useful in designing better drug delivery nanosystems and for understanding of the involved interactions in the relevant biological medium.

2. EXPERIMENTAL DETAILS

Lumichrome (Fluka-Sigma-Aldrich) has been recrystallized from saturated ethanol solution and dried under vacuum prior to use. Control measurement, done in 1,4-dioxane solution, gave a single emission lifetime of 0.45 ns, in agreement with the value reported in ref 16. HSA protein (Fluka-Sigma-Aldrich, 99%) and β-CD (Across Organics, 99%) were used as received. Sodium phosphate buffer 0.1 M at pH 7.0 was used in the preparation of the aqueous samples containing HSA. Aliquots of a KOH water solution were used to set the desired pH of the samples. Steady-state absorption and emission spectra were recorded on JASCO V-670 and Fluoromax-4 (Jobin-Yvone) spectrometers, respectively. The emission lifetimes and anisotropy decays were measured using a previously described picosecond time-correlated single-photon counting spectrophotometer (FluoTime 200).[39] The sample was excited by a 40 ps pulsed (20 MHz) laser centered at the desired wavelength (371, 433, or 470 nm). The emission collected at the magic angle (54.7°) relatively to the excitation, passed through a monochromator and into a fast detector (multichannel plate photomultiplier). A multiexponential function convoluted with the instrument response function (IRF, ~65−90 ps) was globally fitted to the emission decays using the Fluofit package. The time-dependent anisotropy, $r(t)$, was constructed using the decays collected at parallel and perpendicular polarizations of excitation and emission ($I_{\parallel}$, $I_{\perp}$). $r(t) = (I_{\parallel} - GI_{\perp})/(I_{\parallel} + 2GI_{\perp})$, where G is an instrument and wavelength dependent correction factor to compensate for the polarization dependence of the detection system. The G value was calculated for each emission wavelength using the tail-matching technique at enough long time window. The quality of the fits was characterized in terms of the residual distribution and reduced χ^2 values ($\leq$1.2). All the measurements were made at ~293 K.

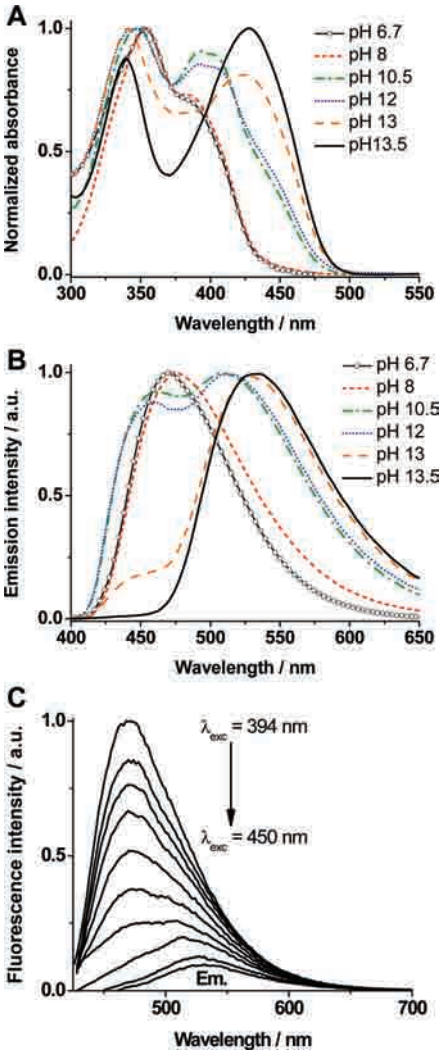

Figure 1. UV−visible (A) absorption and (B) emission spectra of Lc in water at different pH as indicated in the inset. For emission, the excitation wavelength was 370 nm. (C) Emission spectra of 7.4×10^{-6} M of Lc in an aqueous solution of pH 6.7 and exciting at 394, 402, 406, 400, 414, 418, 422, 426, 438, and 450 nm.

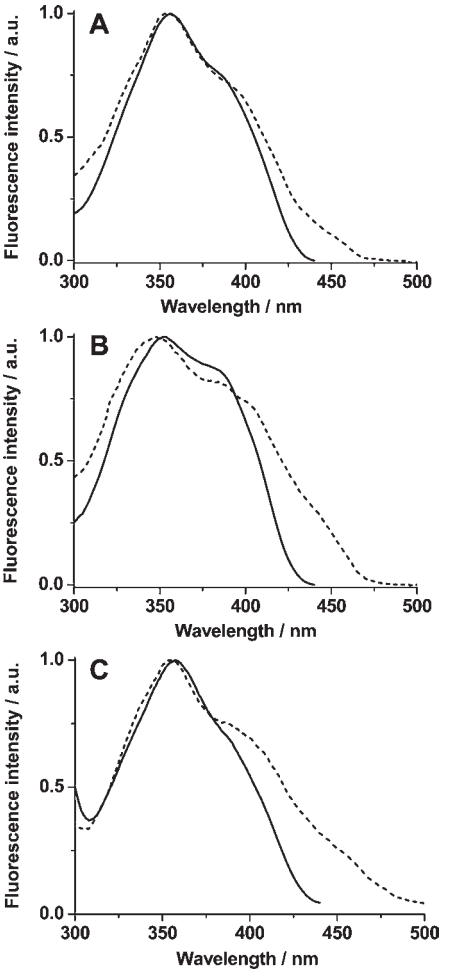

Figure 2. Room temperature fluorescence excitation spectra of (A) 1.4×10^{-5} M of Lc in an aqueous solution of pH 6.7, (B) containing 5 mM of β-CD and (C) 2.1×10^{-5} M of Lc in a water phosphate buffer solution at pH 7 containing 100 μM of HSA protein. The observation wavelengths were at 450 (—) and 570 nm (- - -).

3. RESULTS AND DISCUSSION

3.1. Steady-State Absorption and Emission. *3.1.1. Lc in Water at Different pHs.* The investigation of Lc interactions with caging hosts (CD, HSA) requires determination of the structures present in aqueous solutions. Figure 1 shows the UV−visible absorption and emission spectra at pH 6.7, 8, 10.5, 12, 13, and 13.5. The fluorescence excitation spectra at different pHs are presented in Figure 2A, and in the Supporting Information (Figures S1−S4). From the absorption and emission spectra, three types of behavior of Lc can be distinguished depending on the pH, and therefore showing different Lc structures in solutions.

For water solutions having pH 6.7−8, the absorption spectrum shows the maximum of intensity at about 355 nm, and a shoulder extending to around 390 nm. The tail of the absorption extends to ~450 nm. We assign the 355 and 390 nm absorptions to neutral DMAL form of Lc (Scheme 1). Previously, it has been reported that these bands are due to two independent π,π^* transitions of DMAL form.[40−42] However, results of theoretical calculations suggest that the observed $S_1(\pi,\pi^*)$ of DMAL is close to an (n,π^*) one.[43,44] On the other hand, the presence of the low-energy tail (~450 nm), and the relatively low solubility of Lc in water may suggest formation of dimers. We recorded the absorption, emission spectra, and the fluorescence decay times of Lc having different concentrations in water, 10^{-7} to 10^{-5} M (see Figures S5−S7, Supporting Information), and in THF (10^{-6} to 10^{-4} M). Within our experimental errors, we observed no changes in the fluorescence lifetimes nor in the spectra, except the normal intensity increase with the Lc concentration. This result agrees with previous reports, and Lc dimer formation has been reported only in its solid state.[21,25] In aqueous solutions, H-bonding interactions with water molecules may produce deprotonated (anionic) forms of Lc.[19] A comparison of the absorption and emission spectra with the results obtained at higher pH values, as well as the picosecond time-resolved experiments (vide infra), show that the weak absorption tail at ~450 nm is due to a small population of Lc anion. Nevertheless, at this range of pH the DMAL structure is the dominating specie at S_0.

For the behavior of the electronically first excited state, the fluorescence spectrum (Figure 1B) shows a broad (full width at

dx.doi.org/10.1021/jp110134f |J. Phys. Chem. B 2011, 115, 2424–2435

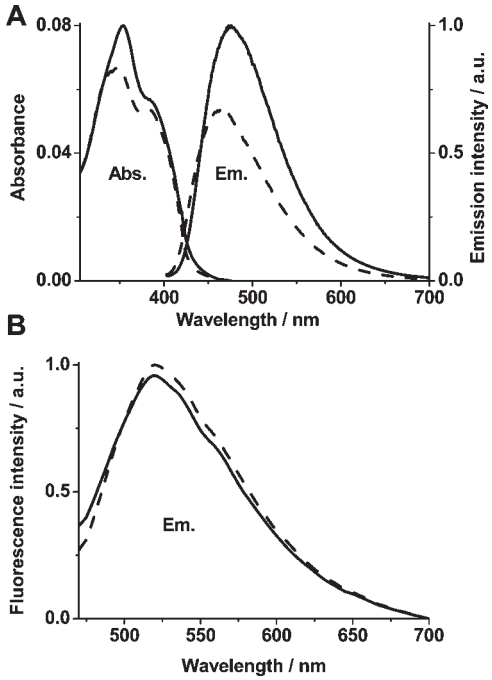

Figure 3. (A) UV−visible absorption (Abs) and emission (Em) spectra of 7.4×10^{-6} M of Lc in aqueous solution of pH 6.7 (—) and in the presence of 5 mM of β-CD (- - -). The excitation wavelength was 350 nm. (B) Emission spectra of 7.4×10^{-6} M of Lc in an aqueous solution of pH 6.7 (—) and in the presence of 5 mM of β-CD (- - -), upon excitation at 450 nm.

half-maximum, fwhm ~4000 cm^{-1}) emission band with the intensity maximum at ~475 nm, and a tail extending to 650 nm. The intensity of this tail is smaller at pH 6.7 than at pH 8 solution. In agreement with previous works,[40,42] the maximum of the emission band is assigned to the fluorescence from the prevailing DMAL form. However, we found that the position and intensity of the emission spectra depend on the excitation wavelength. Figure 1C shows this dependence in water, at pH 6.7, when exciting at different wavelengths. Clearly, the intensity maximum is changing from 475 to 520 nm for 350 and 450 nm excitations, respectively. This evolution shows the presence of two emitting forms in solution, having different absorption and emission spectra. Figure 2A shows the normalized fluorescence excitation spectra of Lc in water at pH ~6.7, monitored at 450 and 570 nm. The shape of the spectrum, observed at 450 nm, agrees well with the absorption one, which indicates that the dominant form of Lc (DMAL) has its emission maximum in this region. In turn, for the long wavelength of observation (570 nm), a significant increase of the shoulder intensity around 430−460 nm is observed in the excitation spectra, indicating that the weak tail in the absorption spectrum is due to a different form of Lc. Based on the reported similarity of the absorption and emission spectra of Lc to those of its derivative having a methyl group at position 1, the presence of an isoalloxazinic tautomer (DMIS, Scheme 1), produced by a water-assisted proton-transfer reaction from nitrogen N-1 to N-10 sites, can be excluded.[11] A previous study has shown the presence of two different monoanions and dianionic structures at higher pH values.[19] In water at pH 6.7 and under our experimental conditions, the red-shifted emission band, observed upon 450 nm excitation (Figure 1C), has a spectral position (~520 nm) similar to that of the low-energy fluorescence band, present

Table 1. Values of the Wavelengths at the Intensity Maxima of UV−Visible Absorption (λ_A/nm) and Fluorescence (λ_F/nm) Spectra of Lumichrome (Lc) in the Indicated Media

		λ_F/nm	
medium	λ_A/nm	λ_{exc} = 350 nm	λ_{exc} = 450 nm
water	354, 385[a]	475	520
water + β-CD	348, 385[a]	465	520
dioxane	327, 379	445	
buffer + HSA	351, 390,[a] 450[a]	500	520

[a] Shoulder.

at pH 10.5, and assigned to the A1 anion structure (Scheme 1).[19] These observations suggest that the weak absorption around 450 nm giving the emission at 520 nm in neutral water is due to a relatively low population of A1, present at the ground state. The intensity difference in the red region of the emission at pH 8 supports this assignment. In turn, the blue emission band possesses a spectral characteristic of the DMAL form of Lc. Time-resolved experiments give further confirmation of both assignments (vide infra).

At pH 10.5−12, the absorption spectrum shows two bands at 350 and 400 nm, and a shoulder at ~450 nm. The emission spectrum (Figure 1B) upon excitation at 370 nm shows now two fluorescence bands having intensity maxima at ~460 and ~515 nm. The spectral changes indicate the predominance of the monoanions. A previous study assigned the low-energy emission to anion A1 and the higher energy one to the anion A2 (Scheme 1).[19] The presence of the two structures is confirmed by the different excitation spectra (Figure S3, Supporting Information) observed at 440 and 550 nm. The result also indicates a lack of excited-state equilibrium between both A1 and A2 anionic structures. At pH 13 and above, the dianionic form (Scheme 1) absorbs at 340 and 430 nm and gives a single fluorescence band at 530 nm. The fluorescence excitation spectra observed at the high and low energy side of the emission band are not different.

In summary, at pH 6.7−8 the most stable form at S_0 is the neutral DMAL with a minor population of anion A1. At pH 10−12, the dominating forms are the anions A1 and A2, showing different absorption and emission spectra. Finally, at pH higher than 13, the dianion is the only populated structure.

3.1.2. Lc in the Presence of β-CD and HSA. Figure 3A shows the UV−visible absorption and emission spectra of 7.4×10^{-6} M Lc in water (at pH 6.7), and of 2.1×10^{-5} M Lc in aqueous buffer in the presence of 5 mM β-CD. Upon addition of β-CD, the intensity of the absorption band centered at 354 nm slightly decreases and a small blue shift is observed (348 nm, Table 1), which is due to the formation of inclusion complexes between β-CD and Lc. The decrease in the absorbance intensity upon addition of CD suggests lower values of the molar extinction coefficients of the complexes in this region. The shift to shorter wavelengths, observed also in solvents of polarity comparable to that of the cyclodextrin interior, like 1,4-dioxane (327 nm), reflects the higher energy of the π,π^* (S_0-S_1) transition of complexed Lc.[16,41] The formation of complexes is in agreement with a previous work, which reported different values of the binding constant for the DMAL form of Lc with β-CD (1:1 complex) of 966 M^{-1} and 491 M^{-1}, using fluorescence quenching and solubility measurements, respectively.[20]

dx.doi.org/10.1021/jp110134f |J. Phys. Chem. B 2011, 115, 2424–2435

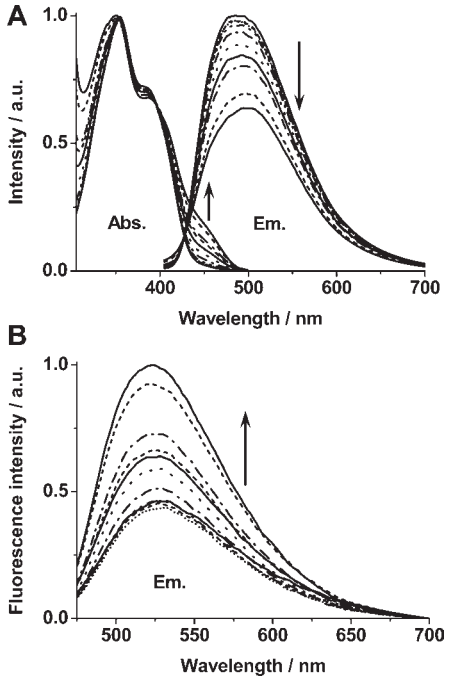

Figure 4. UV−visible absorption (Abs) and emission (Em) spectra of 2.1×10^{-5} M of Lc in a phosphate buffer solution of pH 7 and in the presence of 2.5, 3, 5, 10, 20, 25, 30, 50, 75, and 100 μM HSA protein. The excitation wavelength was (A) 350 and (B) 450 nm. The arrows indicate the changes in the intensity of the corresponding bands with the increase of the HSA protein concentration.

The emission spectrum of Lc in water (pH ∼6.7), excited at 350 nm (Figure 3A), shows a single intensity maximum at ∼475 nm. At this excitation wavelength, the fluorescence is due to the DMAL structure (Scheme 1). Upon addition of β-CD, the emission band decreases its intensity, and is blue-shifted by 10 nm (450 cm^{-1}). As in absorption, both effects reflect the complexation process of Lc with β-CD. The lower fluorescence intensity is partly due to the above-mentioned decrease in the absorbance of the Lc/β-CD solution, but the low polarity of the cavity may participate in this change, decreasing the emission quantum yield of complexed Lc.[12,16] Taking into account the spectral positions of DMAL and the anionic forms of Lc in water (pH 6.7), we explain the blue shift of the emission band, observed for β-CD solutions (Figure 3A) upon excitation at 350 nm, in terms of a preferential complexation of the blue emitting tautomer (DMAL). Into the cavity, this form is less susceptible to deprotonate and the relative contribution of its emission increases, when comparing with that of the anion A1. The emission spectrum of β-CD solutions, excited at 450 nm, is quite similar to that obtained for water (Figure 3B), a result suggesting that the Lc:β-CD complexes do not involve anionic structures.

Figure 4A shows the UV−visible absorption and emission spectra of Lc in a buffer solution at pH 7.0, and in the presence of HSA protein at different concentrations. It is worth noting that upon excitation at 350 nm, the emission spectrum of Lc in a pH 7 buffered solution is centered at ∼490 nm, while in pure water at pH 6.7, the intensity maximum is at ∼475 nm. Additionally, the fwhm of these spectra are ∼4700 and ∼4000 cm^{-1}, respectively. The above differences may be due to different interaction of Lc with the ions present in sodium phosphate buffer ($H_2PO^-_4$/HPO^{2-}_4), when the ionic force in this case is stronger than in pure water. This makes also the anionic form much more stabilized. We will then compare the results obtained in the presence of HSA protein with those in buffered solution not containing the protein.

Upon addition of the protein, the position and intensity of the Lc absorption bands show a small variation (Figure 4 and Table 1). The absorption shoulder at ∼450 nm is much stronger than in the buffer, and its intensity depends on the concentration of the protein (which does not absorb in this region). The position of this band resembles the absorption shoulder, observed in pure water solution (weak) and in alkaline solution at pH 10.5 (much stronger), and we assigned it to the A1 anion. Thus, we attribute the new absorption band to the formation of the complexes between the HSA protein and the A1 anions. The different interactions of Lc with β-CD and HSA are clearly reflected by the emission spectra of the corresponding complexes in both solutions. The addition of HSA protein leads to a decrease in the emission intensity when the excitation wavelength is 350 nm (Figure 4A), while an enhancement in the fluorescence intensity is observed when the excitation is at 450 nm (Figure 4B). Because there is no significant change in the absorption intensity at ∼350 nm, and taking into account the observed decrease in the fluorescence intensity when exciting at 350 nm, we conclude that the complexes involving the protein have a lower fluorescence quantum yield when compared to the free Lc forms. However, the increase in the emission intensity when exciting at 450 nm results from an increase in the absorption intensity at ∼450 nm. For 350 nm excitation, a small red shift in the emission band is observed. This is due to a growing contribution of the long-wavelength emission band. When exciting at 450 nm, the intensity of the band increases, but we do not observe changes in the spectral position (520 nm), nor broadening of the band. The similarity of the emission spectrum in the presence of HSA protein to that in buffer suggests that A1 anions interacting with HSA protein are not significantly changing its electronic structure.

More insight is provided by analyzing the excitation spectra. Their intensity maximum monitored at 450 and 570 nm in water and in HSA protein and β-CD aqueous solutions is at ∼355 nm (Figure 2). The spectra show a shoulder at ∼390 nm, similar to that observed in the absorption spectra. When the fluorescence at the red part of the spectra is collected, a new shoulder is observed at ∼450 nm, and its relative intensity (upon normalization at the maximum) is the largest one for the protein solution. For the latter, the behavior is explained in terms of an increased absorption of anionic structures inside the protein pocket. In β-CD solution, the relatively strong shoulder at 450 nm is probably due to a much larger fluorescence quantum yield of free A1 in solutions than of preferentially complexed DMAL (see fluorescence lifetimes in Table 2).

To obtain the stoichiometry of the complexes with HSA protein, we used Job's plot technique[45] and examined the change in the absorbance of the complex at 455 nm versus the molar fraction of HSA (X_{HSA}) in the solutions. The plot (inset in Figure 5) clearly shows that the maximum of the absorption occurs at $X_{HSA} = 0.5$. Therefore, the complex has a 1:1 stoichiometry. To obtain the binding constant, we took into consideration a fact that the host (HSA) is not in very large excess compared to the guest (Lc). The equilibrium and the equilibrium constant are expressed by the following equations:

$$Lc + HSA \overset{K}{\leftrightarrow} Lc : HSA$$

Table 2. Values of the Fluorescence Lifetimes (τ_i) and Normalized (to 100) Pre-exponential Factors (a_i) Obtained from a Global Multiexponential Fit of the Emission Decays of Lc in an Aqueous Solution (Buffered and Unbuffered), in the Presence of β-CD (5 mM) and HSA Protein (100 μM)[a]

medium	λ_{obs}/nm	τ_1/ns	a_1/%	τ_2/ns	(a_2/%)	τ_3/ns	(a_3/%)	τ_4/ns	(a_4/%)
water pH 6.7	460	4.2	12	2.3	88				
	500		16		84				
	540		22		78				
	580		26		74				
water pH 6.7 + β-CD	460	4.2	0	2.2	26	0.74	74		
	500		4		35		61		
	540		13		37		50		
	580		22		35		43		
buffer pH 7	450	4.6	4	2.3	96				
	475		7		93				
	500		22		76				
	550		75		25				
buffer pH 7 + HSA	450	4.6	5	2.3	53	0.83	15	0.14	27
	475		6		63		13		18
	500		16		52		16		16
	550		45		17		25		13

[a] The excitation wavelength was 371 nm, and the observation ones are indicated in the table.

$$K = \frac{[\text{Lc} : \text{HSA}]}{[\text{Lc}][\text{HSA}]} \quad (1)$$

The concentrations of free Lc and HSA can be described by

$$[\text{Lc}] = [\text{Lc}]_T - [\text{Lc} : \text{HSA}] \quad (2)$$

$$[\text{HSA}] = [\text{HSA}]_T - [\text{Lc} : \text{HSA}] \quad (3)$$

where $[\text{Lc}]_T$ and $[\text{HSA}]_T$ are the total concentrations of Lc and HSA, respectively. Then, the concentration of the complex is given by

$$[\text{Lc} : \text{HSA}] = \frac{([[\text{Lc}]_T + [\text{HSA}]_T + K^{-1}) \pm \sqrt{([\text{Lc}]_T + [\text{HSA}]_T + K^{-1})^2 - (4[\text{Lc}]_T[\text{HSA}]_T)}}{2} \quad (4)$$

The following equations relate the absorbance measurements to the bimolecular equilibrium outlined above:

$$\frac{A_i}{A_S} = \frac{[\text{Lc} : \text{HSA}]_i}{[\text{Lc} : \text{HSA}]_S} = \frac{[\text{Lc} : \text{HSA}]}{[\text{Lc}]_T} \quad (5)$$

$$A_i = \frac{A_S[\text{Lc} : \text{HSA}]}{[\text{Lc}]_T} \quad (6)$$

where A_i is the absorbance change of Lc produced by the binding of increasing quantities (i) of HSA, A_S is the absorbance change of Lc at saturation. $[\text{Lc:HSA}]_i$ is the concentration of the complex as varying quantities (i) of HSA are added to a constant amount of Lc, and $[\text{Lc:HSA}]_S$ is the concentration of the complex at saturation of HSA. Substituting eq 4 in eq 6 yields the final equation:

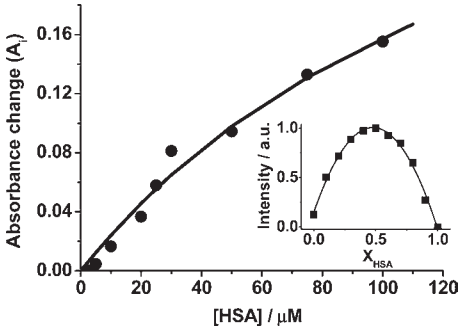

Figure 5. Changes in the absorbance ($A_i = A_{obs} - A_0$, at 455 nm) of Lc (2.1×10^{-5} M) in aqueous solutions upon addition of the HSA protein. The solid line shows the best fit obtained assuming a 1:1 equilibrium of Lc:HSA protein complex using the model described in the text. The inset shows a Job's plot of Lc:HSA protein absorption at 455 nm in an aqueous buffer solution of pH 7 upon increasing the molar fraction of HSA protein (X_{HSA}).

$$A_i = \frac{\{A_S[(K^{-1} + [\text{Lc}]_T + [\text{HSA}]_T) - \sqrt{([\text{Lc}]_T + [\text{HSA}]_T + K^{-1})^2 - (4[\text{Lc}]_T[\text{HSA}]_T)}]\}}{2[\text{Lc}]_T} \quad (7)$$

Figure 5 shows that eq 7 successfully describes the binding behavior of the system, confirming 1:1 binding stoichiometry of the complexes. A K value of 8600 ($\pm$600) M^{-1} is obtained, which gives a $\Delta G° = (-5270 \pm 60)$ cal/mol (at 293 K). The K value is 1 order of magnitude larger than the values (966 and 491 M^{-1}) reported previously for Lc:β-CD complexation.[20]

Summarizing, in the presence of β-CD, the complexed Lc structure is the DMAL form, while for HSA protein solution, the anion A1 is the interacting structure.

3.2. Time-Resolved Fluorescence. To get information on the S_1 relaxation dynamics of Lc forms associated to HSA protein

Table 3. Values of the Fluorescence Lifetimes (τ_i) and Normalized (to 100) Pre-exponential Factors (a_i) Obtained from a Global Multiexponential Fit of the Emission Decays of Lc in Aqueous Solution (Buffered and Unbuffered), in the Presence of β-CD (5 mM) and HSA Protein (100 μM)[a]

medium	λ_{obs}/nm	τ_1/ns	(a_1)	τ_2/ns	(a_2)	τ_3/ns	(a_3)	τ_4/ns	(a_4)
water pH 6.7	475	4.4	20	2.3	80				
	485		24		76				
	530		44		56				
	550		47		53				
	580		53		47				
	600		56		44				
water pH 6.7	475	4.4	24	2.3	32	0.72	44		
+ β-CD	485		39		26		35		
	530		77		5		18		
	550		81		2		17		
	600		73		9		18		
buffer pH 7	475	4.7	11	2.3	89				
	485		21		79				
	530		66		34				
	550		75		25				
	600		77		23				
buffer pH 7	475	4.7	5	2.3	21	0.83	25	0.14	49
+ HSA	485		6		18		34		42
	530		10		15		49		26
	550		12		15		50		23
	580		13		15		51		21
	600		13		14		51		22

[a] The excitation wavelength was 433 nm, and the observation ones are indicated in the table.

and β-CD cavities, we recorded the emission decays in water at different pH, buffer solution (pH 7), and in aqueous solutions containing 5 mM of β-CD and 100 μM of HSA protein. The excitation was done at 371 nm (Table 2, Figure S8A, and Table S2, Supporting Information), 433 nm (Table 3, Figure S8B, Supporting Information), or 470 nm (Table S1, Supporting Information).

3.2.1. Lc Lifetimes in Water at Different pH. The emission decays of Lc in water (pH 6.7, 8), excited at 371 nm, are globally fitted with a biexponential function, giving comparable time components τ_1 and τ_2. At pH 6.7, the time constants are τ_1 = 4.2 and τ_2 = 2.3 ns and are observed through all the gated emission range (460−580 nm). It was mentioned in the Introduction that a single lifetime of 2.4−2.7 ns for Lc in water has been reported in the literature.[11,16,19,20] The value of τ_2 obtained here agrees well with this lifetime. However, under our experimental conditions, the contribution of the 4.2 ns component in the decay is significant at all observation wavelengths, and it increases at the longer ones. For example, the amplitude (normalized pre-exponential factor) for the τ_1 component changes from 12% to 26% at 460 and 580 nm, respectively. The spectral positions and the relative contributions of the τ_1 and τ_2 lifetime components are shown in Figure 6 as decay-associated spectra (DAS), constructed using the stationary emission spectra and the amplitudes shown in Tables 2 and 3 (for λ_{exc} = 371 and 433 nm, respectively). For both wavelengths of excitation, the 2.3 ns component has the intensity maximum at the low-energy side

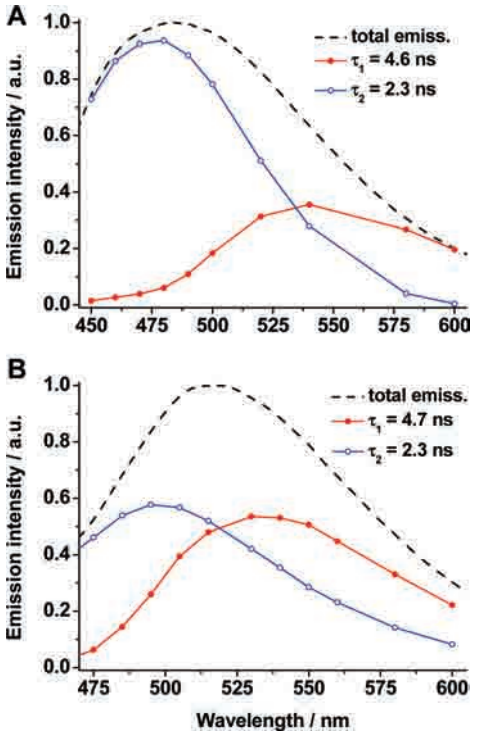

Figure 6. Decay-associated spectra (DAS) of 2.1 × 10^{-5} M LC emission in an aqueous buffer solution at pH 7. The DAS were constructed using stationary fluorescence spectrum (- - -) and normalized pre-exponential factors of (●) τ_1 and (○) τ_2 lifetime components shown in (A) Table 2 and (B) Table 3.

of the spectrum (in the 470−500 nm region), while that of the 4.6−4.7 ns lifetime is found at longer wavelengths, above 525 nm. The relative intensities of DAS spectra of both components depend on the excitation wavelength, being larger for the 2.3 ns lifetime when exciting at the higher energy (371 nm). In agreement with the spectral positions of both components, we assign the 2.3 ns lifetime to the neutral DMAL form, and the 4.2 ns one to the anion A1 fluorescence lifetime. When the solution is a phosphate buffer at pH 7, the value of τ_1 increases to 4.6 ns, while that of the short one stays the same. However, the amplitude of the τ_1 component changes in the buffer and increases to 75% at the red side of the emission spectrum (550 nm). This change can be due to the interactions of the Lc structures with the ions present in the buffer, stabilizing the A1 anionic forms. At pH 8, the two components give τ_1 = 4.0 ns and τ_2 = 2.4 ns, the latter being predominant at all the wavelengths of observation (Table S2, Supporting Information). These times are similar to those obtained in nonbuffered water (pH 6.7), although with a slightly shorter value of τ_1 (4.2 ns). Additionally, the amplitude of τ_1 reaches larger value (33% at 580 nm) than in the case of nonbuffered water at pH 6.7.

At pH 10.5, where the monoanions are the main forms, as we have shown previously (Figure 1), we obtained τ_1 = 4.4 ns and τ_2 = 1.5 ns. The amplitude of τ_1 is very small at the blue side of the emission spectrum (~1% at 450 nm) but prevails at the red side (77% at 580 nm). The increase of the τ_1 amplitude with the pH value (26, 33, and 77% at pH 6.7, 8, and 10.5, respectively, at 580 nm) supports the assignment of this time component as the lifetime of anionic form. For comparison, in a previous study at

pH ~10.3, lifetimes of 1.2 and 4.1 ns have been reported for anions A2 and A1, respectively.[19]

At pH 13.5, the emission decays are clearly monoexponential, giving a time value of 1.6 ns, which is assigned to the dianionic structure. The single fluorescence lifetime present in these conditions agrees with the wavelength-independent fluorescence excitation spectrum in Figure S4 (Supporting Information). Notice that the lifetime value obtained for dianions is similar to that assigned to anion A2, but the spectral positions of these structures are very different (Figure 1B).

We have not observed any rise time component over the monitored emission wavelengths. A rise time could be assigned to an excited-state proton-transfer (ESPT) reaction from DMAL molecules to the solvent (water). Moreover, our femtosecond fluorescence up-conversion experiments (to be published) also do not show any rise components, which could be assigned to the above processes, normally occurring in the ultrafast time scale. These results indicate that the population of the anion A1 observed in water (pH 6.7) at S_0 is directly excited giving a 4.2 ns lifetime component.

3.2.2. Lc lifetimes in the Presence of β-CD and HSA Protein. In the presence of β-CD (5 mM) and exciting at 371 nm, the emission decays are fitted with a three-exponential function, giving lifetimes $\tau_1 = 4.2$ ns, $\tau_2 = 2.2$ ns, and $\tau_3 = 0.74$ ns (Table 2). The first two values (τ_1, τ_2) correspond respectively to the free A1 anion and free DMAL present in water, as assigned above. The time τ_3 is due to emission of 1:1 Lc:β-CD complexes. The amplitude of the τ_3 component changes from 74 to 43%, when we collect the emission from 460 to 580 nm. The larger amplitude of the complexes emission at the blue part of the spectrum indicates that they are formed with neutral DMAL molecules, in agreement with the above discussion, assigning the spectral region of this species. Additionally, Table 2 shows a large decrease of free DMAL amplitude upon complexation with β-CD in favor to the complexes. This change is, however, difficult to quantify due to the three equilibria between DMAL, anion, and complex structures. The shortening of the lifetime of the complexed DMAL is due to a lower polarity and the hydrophobic character of the cyclodextrin cavity. The influence of both these parameters on the photophysics of Lc has been reported, and it is clearly observed when the lifetimes of Lc are compared in different solvents (e.g., for tetrahydrofuran, dioxane, acetonitrile, and methanol the respective lifetime values are 0.36, 0.45, 0.64, and 1.04 ns).[5,9,26] A possible origin of the emission lifetime shortening in less polar solvents is the increase in the nonradiative rate constant caused by a mixing of n,π* and π,π* excited singlet states.[16,43,44,46] In the vacuum, the minimum of the S_1 potential energy surface (PES) of the n,π* electronic structure of DMAL is found below that of the π,π* one, most probably leading to an ultrafast internal conversion and a complete quenching of the fluorescence.[44] However, when the solvent effect is included in the theoretical model, the calculation showed a blue shift of the n,π* state and a red one of the π,π* state. This change will result in a different quenching efficiency of emission from a π,π* state. The π,π* → n,π* crossing is still possible and a relatively short fluorescence lifetime is expected.[44] These effects explain also the reported decrease of the fluorescence quantum yield of Lc (and alloxazines) in comparison to flavins. The observed substantial decrease in the complex lifetime (0.74 ns) in comparison with free DMAL (2.3 ns), in addition to the polarity and H-bonding effects on the lifetime of this structure (see above), suggest that Lc is caged through the heterocyclic ring, as this part of the dye should be more sensitive to the environment changes. In the reverse situation of the inclusion mode (when the dimethylphenyl moiety is the encapsulated part), the heterocyclic ring will be exposed to water, and one can expect little change in the emission lifetime of the complex—a situation we did not observe. Due to the Lc molecule length (~9.5 Å) compared to that of β-CD cavity (~7.9 Å), the embedded Lc is partially accessible to the surrounding water. This is clearly illustrated when the emission spectra of aqueous and dry-solid complexes are compared (see Figures 1A and 3A in ref 14). We observed no evidence of DMAL→DMIS tautomerization upon inclusion within β-CD.

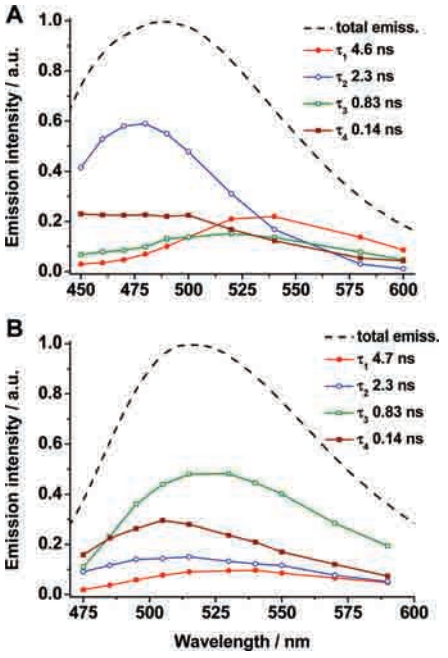

Figure 7. Decay-associated spectra (DAS) of 2.1×10^{-5} M LC emission in an aqueous buffer solution at pH 7 in the presence of 100 μM of HSA protein. The DAS were constructed using stationary fluorescence spectrum (- - -) and normalized pre-exponential factors of (●) τ_1, (○) τ_2, (□) τ_3, and (■) τ_4 lifetime components shown in (A) Table 2 and (B) Table 3.

Upon excitation at 433 nm, the emission decays in water and β-CD solutions give lifetimes similar to those obtained at 371 nm (Table 3). However, in both solutions, and as expected, we observed much larger relative amplitude of fluorescence from free anion A1 when exciting at longer wavelengths, which is due to predominant absorption of the anion A1 in the 430−460 nm region. In aqueous solutions, the influence of an excess of excitation energy (371 vs 433 nm) on the values of the decay times of the relaxed structures is small. However, a substantial decrease in the components amplitude, related to DMAL within β-CD (τ_3) and observed upon 433 nm excitation confirms that this entity absorbs at a different (shorter) wavelength than the anion A1.

In the presence of 100 μM of HSA protein and exciting at 371 nm, three components are not sufficient to accurately fit the decays. Thus, we globally fitted them with a four-exponential function using fixed values of the time constants $\tau_1 = 4.6$ ns and $\tau_2 = 2.3$ ns (lifetimes of the free forms in buffer). This approach allows us to propose a reasonable physical model, while reducing the number of free parameters in a mathematical reconvolution

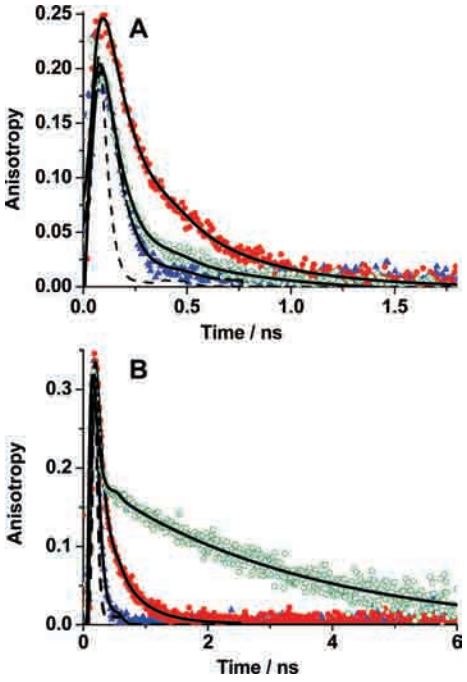

Figure 8. Decays of emission anisotropy of Lc (▲) in buffer solution at pH 7, (○) in the presence of 100 μM of HSA protein, and (●) 5 mM of β-CD at pH 6.7. The instrumental response function (IRF) is indicated with a dashed line and the solid lines are from the best exponential fit. The excitation and observation wavelengths were: (A) λ_{exc} = 371 nm, λ_{obs} = 500 nm; (B) λ_{exc} = 433 nm, λ_{obs} = 550 nm.

procedure. It also gives a good quality of the fits at both short (sub-nanosecond) and long (up to 20 ns) time windows of observation. We obtained τ_3 = 0.83 ns and τ_4 = 0.14 ns. Clearly, these times are related to Lc interacting with the protein, as they are absent in buffer without protein, as well as in a protein solution without Lc. We carefully checked that the short 140 ps component is not due to an artifact or scattered light. The amplitude of τ_3 increases from 15 to 25% while that of τ_4 decreases from 27 to 13%, when we change the observation wavelength from 450 to 550 nm (Table 2). It is interesting to note that the trend in the amplitude variation for the 0.83 ns component in HSA protein solution is opposite to that observed for the τ_3 (0.74 ns) amplitude using β-CD. This trend suggests a different origin of both components even if they give very comparable lifetimes. The spectral positions of the Lc lifetime components τ_1−τ_4 in the presence of the HSA protein are presented in Figure 7 using DAS spectra. The components related to the free Lc in solution (2.3 and 4.7 ns) have positions very similar to those observed in absence of HSA (Figure 6). For the lifetimes of the complexed Lc, the 0.83 ns component shows larger dependence of intensity on the excitation wavelength, being significantly more intense at 433 nm of excitation. The DAS spectrum of this component is broad with an intensity maximum at ~525 nm. However, the 0.14 ns lifetime has its DAS spectrum centered at ~500 nm, with similar intensities for both wavelengths of excitation.

To assign the τ_3 and τ_4 components in the HSA protein solution, we have to consider the following. First, a 1:1 stoichiometry of the complexes was determined from the absorption spectrum (Figure 5). Second, two different emission lifetimes (τ_3 and τ_4) of Lc structures interacting with the HSA protein were obtained. Third, we observed no difference between the τ_3 and τ_4 times when exciting at 371, 433, and 470 nm. Finally, the ratio of the amplitudes (a_3/a_4) of both components due to the complexes does not depend on the excitation wavelength (371, 433, and 470 nm). This last observation reflects one common ground-state form, giving two excited structures having the τ_3 and τ_4 lifetimes. Using a 100 nm difference between the high- and low-energy excitation wavelengths (371 vs 470 nm) and a single absorption band due to the complexation with HSA protein support the above conclusion. A complexation of neutral DMAL using the protein can be ruled out as it is rather unlikely that within HSA protein this form has the same (red-shifted) absorption spectrum like that of anion A1. Thus, the above observations suggest that both τ_3 and τ_4 decay times are due to anion A1/HSA protein complexes, and the different time values are due to different surrounding of the anions within the HSA protein. A specific site heterogeneity in interaction of the anions and HSA protein should be a clue, determining the photodynamical behavior of the guests (see anisotropy results). Thus, the 140 and 830 ps decay times represent the mean lifetimes of two different distributions. The short lifetime values of the complexed forms suggests a hydrophobic environment around the Lc in agreement with the behavior in solvents of different characteristics.[12,16,47] This result shows that Lc is located inside the hydrophobic cavities of one of the binding sites. For the site of complexation, the HSA protein commonly binds guest molecules within two different sites, i.e., site I (subdomain IIA) and site II (subdomain IIIA). Using the present data, we cannot make a direct assignment of site-specific (site I or II) interaction of HSA protein with Lc anions. Notice that the 1:1 stoichiometry of the complexes excludes the possibility of binding within both sites of the protein.

Summarizing, the lifetime of the complexes using β-CD is 0.74 ns, while these using HSA protein are 0.14 and 0.83 ns.

3.3. Time-Resolved Emission Anisotropy. To get information on the rotational dynamics of the complexes formed in HSA protein and β-CD solutions, we performed time-resolved emission anisotropy ($r(t)$) measurements of Lc in water, in the presence of 100 μM of HSA protein and 5 mM of β-CD upon excitation at 371 and 433 nm, and observing at different wavelengths. Figure 8A shows representative $r(t)$ decays, exciting at 371 nm and observing at 500 nm, while Table 4 contains the values of the rotation times obtained from the fits.

In buffered water (pH ~7), the decay fits to a single exponential function, yielding a rotational time of ϕ = 71 ps. Comparable rotational time values have been obtained for dyes of analogous size.[29,46,48−50] Modeling Lc as a prolate ellipsoid, we calculated a rotational relaxation time of 12 and 50 ps under slip- and stick boundary conditions limits, respectively.[51] The experimental value indicates the existence of strong H-bonding interactions between Lc and the surrounding water molecules, affecting its rotational relaxation time. The observation of a unique rotational time for neutral and anionic forms of Lc in solution shows that they have a similar hydrodynamic situation, where the bulk of water molecules is surrounding these species of similar shapes and volumes.

In the presence of β-CD, the anisotropy decay of Lc is fitted to a biexponential function giving ϕ_1 = 110 ps and ϕ_2 = 440 ps. These values do not change significantly with the observed wavelengths (460−580 nm), nor with the excitation wavelengths (Table 4). The shortest time is due to free dye in the solution. Its value (110 ps) is somewhat higher than that obtained in pure

Table 4. Values of the Fluorescence Rotational Times (φ_i) and Normalized (to 100) Pre-exponential Factors (a_i) Obtained from Multiexponential Fits of the Anisotropy Decays of Lc in the Indicated Media[a]

	λ_{exc} = 371 nm					λ_{exc} = 433 nm				
medium	λ_{obs}/nm	φ_1/ps	a_1/%	φ_2/ns	a_2/%	λ_{obs}/nm	φ_1/ps	a_1/%	φ_2/ns	a_2/%
water pH 6.7	460	71	100							
	500									
	540									
	580									
water pH 6.7 + β-CD	460	110	67	0.44	33	475	110	77	0.48	23
	500		66		34	485		79		21
	540		74		26	530		83		17
	580		72		28	550		79		21
buffer pH 7	450	78	100			475	72			
	475					530				
	500					550				
	550					600				
buffer pH 7 + HSA	450	90	97	0.95	3	475	100	46	1.4	54
	475		98		2	530		68	2.7	32
	500		94		6	550		64	3.3	36
	550		86		14	600		63	4.5	37

[a] The excitation and observation wavelengths are as indicated in the table.

water (~71 ps). The difference is explained in terms of an increased viscosity of the medium in the presence of 10^{-3} M of β-CD, as we have previously reported.[50] This time is not very different from the value obtained in dioxane solution (140 ps), which has a viscosity of ~1.4 cP at 293 K. The longest time ϕ_2 (440 ps) is assigned to the global rotational relaxation time of the 1:1 complex. Previously, we reported comparable rotational times for β-CD 1:1 complexes with aromatic molecules of similar sizes: 510 ps for 2-amino-4,5-dimethoxybenzoate (ADMB), 540 ps for 1′-hydroxy-2′-acetonaphthone (HAN):β-CD, and 660 ps for HAN:2,6-di-*O*-methyl-β-CD.[33,34,50]

In the presence of the HSA protein and at 371 nm excitation, the anisotropy decay is also biexponential, with rotational relaxation times ϕ_1 = 90 ps and ϕ_2 = 950 ps, and a largest contribution of the former component (Table 4). The ϕ_1 value is not very different from that obtained for free Lc in buffer (78 ps). The second rotational time ϕ_2 is 1 order of magnitude longer and is due to anion A1 interacting with HSA protein. Notice, however, that the global rotational time of HSA protein is about 20−45 ns.[52,53] Moreover, similar long times (e.g., 45 ± 7 ns for ADMB:HSA protein complex) are obtained if the probe is strongly bound to the hydrophobic pocket of HSA protein.[33] This indicates that a diffusive motion of Lc takes place in the hydrophobic pockets of the protein and its docking is not robust.

Figure 8B shows the $r(t)$ decays when exciting at 433 nm and observing at 550 nm, and Table 4 gives the values of the obtained rotational times and their amplitudes. At this excitation, the values of the rotational relaxation time constants in buffer and β-CD solution are not very different (within the experimental error) from those obtained when exciting at 371 nm. However, in protein solution we observed a strong dependence of the rotational time ϕ_2 on the excitation and observation wavelengths. Exciting at 433 nm and observing at 475 nm, ϕ_2 = 1.4 ns, while it increases to 4.5 ns at 600 nm of observation (Figure S9, Supporting Information). The change indicates a significant heterogeneity in the complexing processes with the protein and the presence of comparable (and overlapping) contributions of two populations of different emitters. We noticed that the wavelength dependence of ϕ_i is in contrast with the observed excitation wavelength independent lifetimes τ_i. This discrepancy in the behavior is due to different factors affecting these photophysical parameters (ϕ_i and τ_i) of Lc neutral and anionic forms. The values of the rotational times of the included anions mainly depend on the degree of hindrance (or viscosity) to rotation in the protein pocket. For the fluorescence lifetimes, the major change is due to specific and nonspecific (H-bonding, polarity, electrostatic) interactions with the neighboring amino acids of HSA. Obviously, fluorophores having the same shape and volume in media of very similar viscosities will not show any change in their rotational times, while the lifetimes can be largely affected. For the protein solution, we have different 1:1 complexes having different degrees of penetration and interactions with the amino acids of HSA. This heterogeneity in interaction, and then in specific anionic populations, will give different rotational times. Moreover, these differently trapped Lc molecules may emit at different wavelengths (Figure 7). Yet, a slow diffusive motion of the guest occurs inside the protein pocket, as the longest ϕ_2 value is at least 4.5 times shorter than the rotational time of the whole protein (~20−45 ns). At 371 nm excitation, this heterogeneity is mostly overlooked due to the weak absorption of the complexes and, therefore, a weak emission when compared to those of the free Lc structures. Upon excitation at the edge of the absorption spectrum, the complex absorption is more significant.

Finally, the initial value of anisotropy $r(0)$ is lower than the theoretical value (0.4) and depends on both excitation and emission wavelengths. The lower $r(0)$ value most probably indicates an ultrafast change in the emission transition moment direction occurring below the temporal resolution of our TCSPC setup. In turn, the wavelength dependence of this parameter is again an indication of the presence of several rotors, showing

different ultrafast depolarization, and absorbing/emitting at different spectral regions.

4. CONCLUSION

Steady-state UV−visible absorption and emission spectra and picosecond time-resolved fluorescence measurements show the confinement effects of β-CD cavity and HSA protein on lumichrome. In buffered water solutions, the emission lifetimes of neutral DMAL and anionic forms are 2.3 and 4.6 ns, respectively. Within the cyclodextrin, an 1:1 DMAL:β-CD complex, emitting at ∼470 nm, is observed, and a shortening of the lifetime (from 2.3 to 0.74 ns) occurs, as a result of the low polarity of the hydrophobic cavity. For the HSA protein solution, we determined an 1:1 stoichiometry of the complexes and a binding constant K = 8600 (±600) M^{-1} at 293 K. The protein induces formation of significant population of anionic form of Lc at the ground state. The two lifetime components obtained for the complexes (0.14 and 0.83 ns) are assigned to the Lc anions, differently interacting with the HSA protein residues. Picosecond time-resolved anisotropy experiments confirm the heterogeneity of the binding of Lc to HSA protein, while for the β-CD complexes we only observed one kind of complexes. The results provide information for a better understanding of the lumichrome interactions with water at different pHs and its interactions with CD and the HSA protein. They can be used in the drug delivery and release nanosystems.

■ ASSOCIATED CONTENT

Supporting Information. Values of the fluorescence lifetimes and decays of emission anisotropy of Lc in HSA solutions, concentration dependent absorption, emission and fluorescence decays in water, and fluorescence excitation spectra of Lc at different pH. This material is available free of charge via the Internet at http://pubs.acs.org.

■ AUTHOR INFORMATION

Corresponding Author

*E-mail: Abderrazzak.Douhal@uclm.es.

■ ACKNOWLEDGMENT

This work was supported by the JCCM, MICINN, and FP7 through projects PCI08-5868, MAT2008-01609, CTQ06-0657, and CYCLON Network (MRTN-CT-2008-Project 237962), respectively. M.J.M. and C.M. thank the MICINN for their fellowships.

■ REFERENCES

(1) Müller, F., Ed. *Chemistry and Biochemistry of Flavoenzymes*; CRC Press: Boca Raton, FL, 1990−1991; Vols. I−III.
(2) Sancar, A. *Chem. Rev.* **2003**, *103*, 2203–2237.
(3) Kao, Y.-T.; Saxena, C.; He, T.-F.; Guo, L.; Wang, L.; Sancar, A.; Zhong, D. *J. Am. Chem. Soc.* **2008**, *130*, 13132–13139.
(4) Massey, V. *Biochem. Soc. Trans.* **2000**, *28*, 283–296.
(5) Ghisla, S.; Massey, V. *Eur. J. Biochem.* **1989**, *181*, 1–17.
(6) Phillips, D. A.; Joseph, C. M.; Yang, G.-P.; Martinez-Romero, E.; Sanborn, J. R.; Volpin, H. *Proc. Natl Acad. Sci. U. S. A.* **1999**, *96*, 12275–12280.
(7) Ueno, K.; Natori, S. *J. Biol. Chem.* **1987**, *262*, 12780–12784.
(8) Tsukamoto, S.; Kato, H.; Hirota, H.; Fusetani, N. *Eur. J. Biochem.* **1999**, *264*, 785–789.
(9) Said, H. M.; Ortiz, A.; Ma, T. Y.; McCloud, E. *J Cell Physiol.* **1998**, *176*, 588–594.
(10) Fieschi, F.; Niviere, V.; Frier, C.; Decout, J.-L.; Fontecave, M. *J. Biol. Chem.* **1995**, *270*, 30392–30400.
(11) Sikorski, M.; Sikorska, E.; Koziołowa, A.; Gonzalez Moreno, R.; Bourdelande, J. L.; Steerd, R. P.; Wilkinson, F. *J. Photochem. Photobiol. B: Biol.* **2001**, *60*, 114–119.
(12) Sikorska, E.; Sikorski, M.; Steer, R. P.; Wilkinson, F.; Worrall, D. R. *J. Chem. Soc., Faraday Trans.* **1998**, *94*, 2347–2353.
(13) Joshi, P. C. *J. Biochem. Biophys.* **1989**, *26*, 186–189.
(14) Sikorski, M.; Prukała, D.; Insińska-Rak, M.; Khmelinskii, I.; Worrall, D. R.; Williams, S. L.; Hernando, J.; Bourdelande, J. L.; Koput, J.; Sikorska, E. *J. Photochem. Photobiol. A* **2008**, *200*, 148–160.
(15) Kozioł, J. *J. Photochem. Photobiol.* **1966**, *5*, 41–54.
(16) Sikorska, E.; Khmelinskii, I. V.; Prukała, W.; Williams, S.; Patel, M.; Worrall, D. R.; Bourdelande, J. L.; Koput, J.; Sikorski, M. *J. Phys. Chem. A* **2004**, *108*, 1501–1508.
(17) Miskolczy, Z.; Biczok, L. *Chem. Phys. Lett.* **2005**, *411*, 238–242.
(18) Miskolczy, Z.; Biczok, L.; Gorner, H. *J. Photochem. Photobiol. A: Chem.* **2009**, *207*, 47–51.
(19) Lasser, N.; Feitelson, J. *Photochem. Photobiol.* **1977**, *25*, 451–456.
(20) Sarkar, B.; Das, U.; Bhattacharyya, S.; Bose, S. K. *Bull. Chem. Soc. Jpn.* **1995**, *68*, 1807–1809.
(21) Mir, M.; Sikorska, E.; Sikorski, M.; Wilkinson, F. *J. Chem. Soc., Perkin Trans. 2* **1997**, 1095–1098.
(22) Uritski, A.; Presiado, I; Huppert, D. *J. Phys. Chem. C* **2009**, *113*, 7870.
(23) Uritski, A.; Presiado, I; Huppert, D. *J. Phys. Chem. C* **2008**, *112*, 18189.
(24) Sikorska, E.; Khmelinskii, I. V.; Kubicki, M.; Prukała, W.; Nowacka, G.; Siemiarczuk, A.; Koput, J.; Ferreira, L. F. V.; Sikorski, M. *J. Phys. Chem. A* **2005**, *109*, 1785–1794.
(25) Sikorska, E.; Khmelinskii, I. V.; Kubicki, M.; Prukała, W.; Hoffman, M.; Machado, I. F.; Ferreira, L. F. V.; Karolczak, J.; Worral, D. R.; Krawczyk, A.; Insińska-Rak, M.; Sikorski, M. *J. Phys. Chem. A* **2006**, *110*, 4638.
(26) Mewies, M.; McIntire, W. S.; Scrutton, N. S. *Protein Sci.* **1998**, *7*, 7–20.
(27) Grininger, M.; Zeth, K.; Oesterhelt, D. *J. Mol. Biol.* **2006**, *357*, 842–857.
(28) Douhal, A.; Sanz, M.; Tormo, L. *Proc. Natl. Acad. Sci. U. S. A.* **2005**, *102*, 18807.
(29) Zhong, D.-P.; Douhal, A.; Zewail, A. H. *Proc. Natl. Acad. Sci. U. S. A.* **2000**, *97*, 14056–14061.
(30) Garcia-Ochoa, I.; Lopez, M. D.; Vinas, M. H.; Santos, L.; Ataz, E. M.; Amat-Guerri, F.; Douhal, A. *Chem.—Eur. J.* **1999**, *5*, 897–901.
(31) Cohen, B.; Organero, J. A.; Santos, L.; Rodriguez Padial, L.; Douhal, A. *J. Phys. Chem. B* **2010**, *114*, 14787–14795.
(32) El-Kemary, M.; Gil, M.; Douhal, A. *J. Med. Chem.* **2007**, *50*, 2896.
(33) Tormo, L.; Organero, J. A.; Cohen, B.; Martin, C.; Santos, L.; Douhal, A. *J. Phys. Chem. B* **2008**, *112*, 13641.
(34) Organero, J. A.; Martin, C.; Cohen, B.; Douhal, A. *Langmuir* **2008**, *24*, 10352–10357.
(35) He, X. M.; Carter, D. C. *Nature* **1992**, *358*, 209–215.
(36) Carter, D. C.; Ho, J. X. *Adv. Protein Chem.* **1994**, *45*, 153–203.
(37) Wardell, M.; Wang, Z.; Ho, J. X.; Robert, J.; Ruker, F.; Ruble, J.; Carter, D. C. *Biochem. Biophys. Res. Commun.* **2002**, *291*, 813–819.
(38) Monti, S.; Manet, I.; Manoli, F.; Marconi, G. *Phys. Chem. Chem. Phys.* **2008**, *10*, 6597–6606.
(39) Organero, J. A.; Tormo, L.; Douhal, A. *Chem. Phys. Lett.* **2002**, *363*, 409–414.
(40) Sun, M.; Moore, T. A.; Song, P. S. *J. Am. Chem. Soc.* **1972**, *94*, 1730.

(41) Song, P. S.; Sun, M.; Koziołowa, A.; Kozioł, J. *J. Am. Chem. Soc.* **1974**, *96*, 4319–4322.
(42) Koziołowa, A. *Photochem. Photobiol.* **1979**, *29*, 459.
(43) Sikorska, E.; Khmelinskii, I. V.; Hoffman, M.; Machado, I. F.; Ferreira, L. F. V.; Dobek, K.; Karolczak, J.; Krawczyk, A.; Insińska-Rak, M.; Sikorski, M. *J. Phys. Chem. A* **2005**, *109*, 11707–11714.
(44) Salzmann, S.; Marian, Ch. M. *Photochem. Photobiol. Sci.* **2009**, *8*, 1655–1666.
(45) Job, P. *Ann. Chim.* **1928**, *10*, 113–203.
(46) Sikorska, E.; Khmelinskii, I. V.; Koput, J.; Bourdelande, J. L.; Sikorski, M. *J. Mol. Struct.* **2004**, *697*, 137–141.
(47) Bertolotti, S. G.; Previtali, C. M.; Rufs, A. M.; Encinas, M. V. *Macromolecules* **1999**, *32*, 2920.
(48) Balabai, N.; Linton, B.; Napper, A.; Priyadarshy, S.; Sukharevsky, A. P.; Waldeck, D. H. *J. Phys. Chem. B* **1998**, *102*, 9617–9624.
(49) El-Kemary, M.; Organero, J. A.; Santos, L.; Douhal, A. *J. Phys. Chem. B* **2006**, *110*, 14128–14134.
(50) Tormo, L.; Organero, J. A.; Douhal, A. *J. Phys. Chem. B* **2005**, *109*, 17848–17854.
(51) Lu, C.; Hsieh, R. M. R.; Lee, I. R.; Cheng, P. Y. *Chem. Phys. Lett.* **1999**, *310*, 103–110.
(52) Marzola, P.; Gratton, E. *J. Phys. Chem.* **1991**, *95*, 9488–9495.
(53) Ferrer, M. L.; Duchowicz, R.; Carrasco, B.; Garcia de la Torre, J.; Acuna, A. U. *Biophys. J.* **2001**, *80*, 2422–2430 and references therein.